JCTC Journal of Chemical Theory and Computation

ARTICLE

pubs.acs.org/JCTC

# Efficient and Accurate Methods for the Geometry Optimization of Water Clusters: Application of Analytic Gradients for the Two-Body:Many-Body QM:QM Fragmentation Method to $(H_2O)_n$, $n = 3-10$

Desiree M. Bates, Joshua R. Smith, and Gregory S. Tschumper*

Department of Chemistry and Biochemistry, University of Mississippi, University, Mississippi 38677, United States

Supporting Information

**ABSTRACT:** The structures of more than 70 low-lying water clusters ranging in size from $(H_2O)_3$ to $(H_2O)_{10}$ have been fully optimized with several different quantum mechanical electronic structure methods, including second-order Møller−Plesset perturbation theory (MP2) in conjunction with correlation consistent triple-ζ basis sets (aug-cc-pVTZ for O and cc-pVTZ for H, abbreviated haTZ). Optimized structures obtained with less demanding computational procedures were compared to the MP2/haTZ ones using both MP2/haTZ single point energies and the root-mean-square (RMS) deviations of unweighted Cartesian coordinates. Based on these criteria, B3LYP/6-31+G(d,2p) substantially outperforms both HF/haTZ and MP2/6-31G*. B3LYP/6-31+G(d,2p) structures never deviate from the MP2/haTZ geometries by more than 0.44 kcal mol$^{-1}$ on the MP2/haTZ potential energy surface, whereas the errors associated with the HF/haTZ and MP2/6-31G* structures grow as large as 12.20 and 2.98 kcal mol$^{-1}$, respectively. The most accurate results, however, were obtained with the two-body:many-body QM:QM fragmentation method for weakly bound clusters, in which all one- and two-body interactions are calculated at the high-level, while a low-level calculation is performed on the entire cluster to capture the cooperative effects (nonadditivity). With the haTZ basis set, the MP2:HF two-body:many-body fragmentation method generates structures that deviate from the MP2/haTZ ones by 0.01 kcal mol$^{-1}$ on average and not by more than 0.03 kcal mol$^{-1}$.

## 1. INTRODUCTION

Hydrogen bonding is widely studied, particularly in water, because of its key roles in biological phenomena as well as in a plethora of important chemical and physical processes.[1−7] The characterization of molecular clusters with sophisticated quantum mechanical (QM) electronic structure techniques is often highly desirable.[8−21] High-accuracy computational procedures are frequently necessary to reliably describe the properties (e.g., structures and energetics) of weakly bound clusters. Such computations can also help unravel the chemical physics of the noncovalent interactions that hold the clusters together. Unfortunately, the computational demands of the most reliable QM methods scale steeply with the size of the cluster, thereby prohibiting their routine application to large systems.

A wide variety of computational techniques have been introduced that partition a cluster into fragments (not necessarily monomers) in an attempt to extend high-accuracy computational methods to previously inaccessible size regimes.[22−42] The integrated QM:QM fragmentation methods being developed by our group fall into this category, and they facilitate the computation of not only energies but also properties. In this paper, we review the two-body:many-body fragmentation method and its analytic gradients. The technique is then used to optimize the geometries of more than 70 $(H_2O)_n$ clusters where $n = 3-10$. The errors associated with these two-body:many-body optimized structures are assessed and compared to those obtained with three other relatively inexpensive electronic structure methods.

## 2. THEORETICAL BACKGROUND

Through careful application of the inclusion−exclusion principle, integrated computational chemistry methods (QM:QM, QM:MM, ONIOM, etc.) have been extended from systems with a single chemically important subset (or reaction center) to systems with an arbitrary number of subsets that can overlap.[43,44] With this "multicentered" approach to integrated computations, the traditional many-body energy decomposition for weakly bound clusters has been recast[45,46] in the ONIOM formalism of Morokuma and co-workers.[47] The result is effectively a QM:QM fragmentation scheme for noncovalent clusters. This basic mathematical principle is also employed by other fragmentation methods, such as (cardinality guided) molecular tailoring,[35,48] generalized energy-based fragmentation,[49,50] and the molecules-in-molecules approach.[51]

In the original two-body:many-body implementation,[45,46] an accurate but computationally demanding high-level QM method is employed to compute the one- and two-body interactions within a cluster, while a less demanding low-level QM method is used to recover the higher-order (≥three-body) interactions, which are also commonly referred to as the cooperative or nonadditive effects. Consequently, a high-level calculation on the entire cluster $[f_1 f_2 \ldots f_n]$ can be avoided, and high-level computations only need to be performed on the fragments $[f_i]$ and unique pairs

**Received:** March 14, 2011
**Published:** August 02, 2011

of fragments $[f_i f_j]$ in the cluster. An expression for the total energy of the cluster can then be obtained by combining the high-level electronic energies with low-level computations on the entire cluster as well as the fragments and pairs:

$$E^{2bHi:Lo} = E_{Lo}[f_1 f_2 \ldots f_n] + \sum_{i=1}^{n}\sum_{j>i}^{n}(E_{Hi}[f_i f_j] - E_{Lo}[f_i f_j]) - (n-2)\sum_{i=1}^{n}(E_{Hi}[f_i] - E_{Lo}[f_i]) \quad (1)$$

When an appropriate low-level method is used (i.e., one that accurately reproduces the high-level ≥three-body effects), the method is quite accurate, and errors typically do not exceed 0.2 kcal $mol^{-1}$. It is also quite efficient because the demands of the high-level computations only increase quadratically with the size of the cluster and are ideally suited for coarse-grained parallelization. An analogous three-body:many-body procedure has also been developed to examine the convergence of the series:[52]

$$\Delta E^{3bHi:Lo} = E_{Lo}[f_1 f_2 \ldots f_n] + \sum_{i=1}^{n}\sum_{j>i}^{n}\sum_{k>j}^{n}(E_{Hi}[f_i f_j f_k] - E_{Lo}[f_i f_j f_k]) - (n-3)\sum_{i=1}^{n}\sum_{j>i}^{n}(E_{Hi}[f_i f_j] - E_{Lo}[f_i f_j]) + \frac{(n-2)(n-3)}{2}\sum_{i=1}^{n}(E_{Hi}[f_i] - E_{Lo}[f_i]) \quad (2)$$

For the three-body:many-body CCSD(T):MP2 approach, errors tend to decrease by an order of magnitude relative to the two-body:many-body method, suggesting that the series quickly converges and that the error can be systematically controlled.

These QM:QM fragmentation schemes have been developed within the ONIOM framework to facilitate the computation of properties, not just energies. An extremely important feature of the expression for cluster energies in eqs 1 and 2 is that they are linear with respect to the computed energies. Consequently for a linear operator like the gradient, one obtains analogous expressions for the gradient by taking linear combinations of the appropriate components from a series of high- and low-level gradient calculations. For example, the two-body:many-body gradient can be expressed in the following manner:

$$\nabla E^{2bHi:Lo} = \nabla E_{Lo}[f_1 f_2 \ldots f_n] + \sum_{i=1}^{n}\sum_{j>i}^{n}(\nabla E_{Hi}[f_i f_j] - \nabla E_{Lo}[f_i f_j]) - (n-2)\sum_{i=1}^{n}(\nabla E_{Hi}[f_i] - \nabla E_{Lo}[f_i]) \quad (3)$$

Evaluation of these two-body:many-body Cartesian gradients is fairly straightforward as long as all gradients are rotated into the same reference frame. The high- and low-level gradients for the fragments $[f_i]$ and pairs $[f_i f_j]$ in eq 3 only contribute to a few components of the composite Cartesian gradient. If atom $a$ is contained in fragment $j$, then the only nonzero contributions to the component of the Cartesian gradient along the $R$ coordinate ($R = x,y,z$) of atom $a$ can be obtained with the following expression:

$$\frac{\partial E^{2bHi:Lo}}{\partial R_a} = \frac{\partial E_{Lo}[f_1 f_2 \ldots f_n]}{\partial R_a} + \sum_{i\neq j}^{n}\left(\frac{\partial E_{Hi}[f_i f_j]}{\partial R_a} - \frac{\partial E_{Lo}[f_i f_j]}{\partial R_a}\right) - (n-2)\left(\frac{\partial E_{Hi}[f_j]}{\partial R_a} - \frac{\partial E_{Lo}[f_j]}{\partial R_a}\right) \quad (4)$$

These analytic gradients were originally implemented in a stand-alone interface to the MPQC ab initio software package[53] and applied to the geometry optimization of 15 different hydrogen-bonded clusters of hydrogen fluoride, water, and methanol.[54] In the current implementation, Cartesian gradients are computed with MPQC, rotated into a common reference frame, and combined to form a composite two-body:many-body gradient that is then passed to the Gaussian 03 optimizer via the "external" keyword.

## 3. COMPUTATIONAL METHODS

All water clusters were optimized with the Hartree−Fock (HF) and second-order Møller−Plesset perturbation theory (MP2) methods, the MP2:HF QM:QM fragmentation method, and the B3LYP density functional. Residual Cartesian gradients of all optimized structures were smaller than $4.5 \times 10^{-4}$ $E_h$ $a_0^{-1}$. The 6-31+G(d,2p) basis set was used with the B3LYP optimizations because it has been shown that this methodology provides quite accurate structures for $(H_2O)_6$ isomers.[55] All B3LYP computations used a pruned grid, composed of 99 radial shells and 590 angular points per shell. Both HF and MP2 optimizations were performed with a triple-ζ correlation consistent basis set, aug-cc-pVTZ for O and cc-pVTZ for H (henceforth denoted haTZ). MP2 optimizations were also performed with the 6-31G* basis set, a prescription that has been used to accurately predict the energetics of cluster formation for the same range of water clusters that are the focus of this study.[56] The QM:QM fragmentation optimizations employed MP2/haTZ as the high-level method and HF/haTZ for the low-level calculations.

For all computations, the change in the root-mean-square (RMS) density between self-consistent field (SCF) iterations was converged to at least $1 \times 10^{-8}$, yielding energies converged to approximately $1 \times 10^{-10}$ $E_h$. The 1s-like core orbitals of the oxygen atoms were frozen in all MP2 calculations. All atomic orbital basis sets employed in this work utilized spherical harmonic functions (5d, 7f) rather than their Cartesian counterparts (6d, 10f). MP2/haTZ single point energy calculations were performed on all optimized structures to compare the relative energies on the MP2/haTZ potential energy surface (PES). All calculations were performed with the Gaussian 03,[57] Gaussian 09,[58] and MPQC[53] software packages.

## 4. RESULTS AND DISCUSSION

Two independent means were used to compare the optimized structures obtained with the various computational methods. The first and more straightforward comparison utilized the minimal RMS deviation of the unweighted Cartesian coordinates optimized with the superpose program in TINKER.[59,60] The second metric is based on energetics. MP2/haTZ single point energies were computed for all optimized structures. By definition, the MP2/haTZ optimized structure corresponds to the lowest point associated with a particular minimum on the MP2/haTZ

**Table 1. RMS Deviations (in Å) for Optimized Structures Relative to the MP2/haTZ Optimized Structures**

| method | HF | MP2 | B3LYP | MP2:HF |
|---|---|---|---|---|
| basis Set | haTZ | 6-31G* | 6-31+G(d,2p) | haTZ |
| | | $(H_2O)_3$ | | |
| $C_1$ | 0.121 | 0.127 | 0.010 | 0.004 |
| $C_3$ | 0.160 | 0.186 | 0.012 | 0.004 |
| $C_{3h}$ | 0.083 | 0.014 | 0.009 | 0.002 |
| | | $(H_2O)_4$ | | |
| $S_4$ | 0.131 | 0.059 | 0.017 | 0.006 |
| $C_i$ | 0.146 | 0.093 | 0.010 | 0.007 |
| $C_4$ | 0.204 | 0.150 | 0.010 | 0.007 |
| $C_{4h}$ | 0.095 | 0.019 | 0.012 | 0.003 |
| | | $(H_2O)_5$ | | |
| $C_1$ | 0.160 | 0.126 | 0.041 | 0.013 |
| $C_5$ | 0.243 | 0.136 | 0.014 | 0.011 |
| $C_{5h}$ | 0.113 | 0.025 | 0.018 | 0.006 |
| | | $(H_2O)_6$ | | |
| prism | 0.147 | 0.081 | 0.031 | 0.011 |
| cage | 0.180 | 0.115 | 0.040 | 0.008 |
| book 1 | 0.203 | 0.076 | 0.020 | 0.008 |
| book 2 | 0.262 | [a] | 0.081 | 0.017 |
| bag | 0.192 | [b] | 0.055 | 0.010 |
| boat 1 | 0.297 | 0.332 | 0.078 | 0.038 |
| boat 2 | 0.304 | 0.280 | 0.080 | 0.015 |
| cyclic | 0.154 | 0.134 | 0.017 | 0.012 |
| | | $(H_2O)_7$ | | |
| A | 0.173 | 0.103 | 0.036 | 0.007 |
| B | 0.196 | 0.399 | 0.039 | 0.009 |
| C | 0.274 | 0.330 | 0.046 | 0.012 |
| D | 0.328 | 0.255 | 0.048 | 0.024 |
| PR2 | 0.178 | 0.131 | 0.047 | 0.009 |
| PR3 | 0.217 | 0.145 | 0.036 | 0.038 |
| CA1 | 0.242 | 0.010 | 0.029 | 0.010 |
| CA2 | 0.386 | 0.174 | 0.025 | 0.011 |
| CH1 | 0.292 | 0.320 | 0.101 | 0.019 |
| BI1 | 0.465 | 0.280 | 0.020 | 0.015 |
| CH2 | 0.235 | 0.294 | 0.043 | 0.015 |
| $(H_2O)_8$ | | | | |
| $C_1$a | 0.166 | 0.073 | 0.029 | 0.010 |
| $C_1$b | 0.167 | 0.068 | 0.030 | 0.009 |
| $C_1$c | 0.173 | 0.070 | 0.029 | 0.007 |
| $C_2$ | 0.186 | 0.021 | 0.050 | 0.006 |
| $C_i$ | 0.200 | 0.050 | 0.031 | 0.004 |
| $C_s$ | 0.179 | 0.076 | 0.032 | 0.007 |
| $D_{2d}$ | 0.164 | 0.068 | 0.024 | 0.009 |
| noncubic 1 | 0.272 | 0.308 | 0.184 | 0.013 |
| $S_4$ | 0.165 | 0.069 | 0.026 | 0.008 |
| | | $(H_2O)_9$ | | |
| $D_{2d}$DDh | 0.184 | 0.091 | 0.025 | 0.009 |
| $S_4$Dah 1 | 0.185 | 0.092 | 0.024 | 0.008 |
| $S_4$Dah 2 | 0.192 | 0.107 | 0.025 | 0.010 |
| $S_4$DDh 1 | 0.184 | 0.103 | 0.026 | 0.010 |
| $S_4$DDh 2 | 0.187 | 0.101 | 0.025 | 0.008 |
| $D_{2d}$Dah | 0.183 | 0.102 | 0.022 | 0.007 |
| $S_4$Danh 1 | 0.185 | 0.125 | 0.023 | 0.008 |
| $S_4$Danh 2 | 0.187 | 0.089 | 0.024 | 0.010 |
| | | $(H_2O)_{10}$ | | |
| PP1 | [c] | 0.073 | 0.029 | 0.013 |
| PP2 | 0.185 | 0.076 | 0.026 | 0.007 |
| PP3 | 0.186 | 0.087 | 0.027 | 0.021 |
| PP4 | 0.191 | 0.084 | 0.028 | 0.007 |
| PP5 | 0.185 | 0.086 | 0.026 | 0.009 |
| OB1 | 0.200 | 0.096 | 0.026 | 0.011 |
| OB2 | 0.202 | 0.094 | 0.028 | 0.008 |
| OB3 | 0.201 | 0.089 | 0.028 | 0.010 |
| DP1 | [d] | 0.102 | 0.028 | 0.008 |
| OB4 | 0.202 | 0.083 | 0.034 | 0.015 |
| OB5 | 0.200 | 0.203 | 0.023 | 0.012 |
| DP2 | 0.190 | 0.109 | 0.033 | 0.008 |
| OB6 | 0.204 | 0.106 | 0.037 | 0.017 |
| OB7 | 0.205 | 0.070 | 0.033 | 0.016 |
| OB8 | 0.205 | 0.073 | 0.032 | 0.014 |
| DP3 | 0.204 | 0.203 | 0.060 | 0.010 |
| DP4 | 0.210 | 0.081 | 0.102 | 0.025 |
| DP5 | 0.204 | 0.089 | 0.050 | 0.014 |
| DP6 | 0.198 | 0.199 | 0.022 | 0.009 |
| OB9 | 0.220 | 0.221 | 0.031 | 0.012 |
| DP7 | 0.225 | 0.143 | 0.032 | 0.011 |
| DP8 | 0.208 | 0.120 | 0.052 | 0.013 |
| OB10 | 0.199 | 0.318 | 0.030 | 0.006 |
| OB11 | 0.284 | 0.279 | 0.043 | 0.018 |
| DP10 | 0.210 | 0.103 | 0.065 | 0.022 |
| DP11 | 0.212 | 0.118 | 0.026 | 0.014 |
| C1 | 0.233 | 0.100 | 0.035 | 0.012 |
| C2 | 0.199 | 0.101 | 0.033 | 0.024 |
| C3 | 0.222 | 0.122 | 0.039 | 0.020 |

[a] Collapsed to prism structure. [b] Not located on the MP2/6-31G* PES. [c] Not located on the HF/haTZ PES. [d] Collapsed to DP2 structure.

PES. All other optimized structures lie above that minimum. Optimization procedures that most accurately reproduce the MP2/haTZ optimized structure will lie closest to the bottom of the well and, therefore, also have the smallest deviation from the MP2/haTZ//MP2/haTZ cluster energy.

All trimer, tetramer, and pentamer structures are commonly studied low-lying stationary points. Hexamer structures were taken from ref 21. Most initial heptamer, octamer, nonamer, and decamer structures came from MP2/6-31G* optimized geometries[56] with a few additional structures from HF/6-31G(d) optimizations.[60] The BI2, BI3, and CH3 isomers of $(H_2O)_7$ along with DP9 of the $(H_2O)_{10}$ have been omitted because they could not be located on the MP2/haTZ PES. We note, however, that exhaustive searches were not performed because they collapse to other structures on the PES. Because the number of possible

**Table 2. Average and Maximum RMS Deviations (in Å) for Various Optimized Structures Relative to the MP2/haTZ Optimized Structures for Various $(H_2O)_n$ Clusters with $n = 3-10$**

| | | HF/haTZ | | MP2/6-31G* | | B3LYP/ 6-31+G(d,2p) | | MP2:HF/ haTZ | |
|---|---|---|---|---|---|---|---|---|---|
| *n* | no. | avg | max | avg | max | avg | max | avg | max |
| 3 | 3 | 0.121 | 0.160 | 0.109 | 0.186 | 0.011 | 0.012 | 0.003 | 0.004 |
| 4 | 4 | 0.144 | 0.204 | 0.080 | 0.150 | 0.012 | 0.017 | 0.006 | 0.007 |
| 5 | 3 | 0.172 | 0.243 | 0.096 | 0.136 | 0.024 | 0.041 | 0.010 | 0.013 |
| 6 | 8 | 0.218 | 0.304 | 0.170[a] | 0.332[a] | 0.050 | 0.081 | 0.015 | 0.038 |
| 7 | 11 | 0.272 | 0.465 | 0.230 | 0.399 | 0.043 | 0.101 | 0.015 | 0.038 |
| 8 | 9 | 0.186 | 0.272 | 0.089 | 0.308 | 0.048 | 0.184 | 0.008 | 0.013 |
| 9 | 8 | 0.186 | 0.192 | 0.101 | 0.125 | 0.024 | 0.026 | 0.009 | 0.010 |
| 10 | 29 | 0.207[b] | 0.284 | 0.125 | 0.318 | 0.037 | 0.102 | 0.013 | 0.025 |

[a] Excludes the bag and book 2 isomers. [b] Excludes the PP1 and DP1 isomers.

configurations grows very quickly with *n*, only structures within 5 kcal mol$^{-1}$ of the lowest-lying isomer were examined in this study.

**4.1. Comparison of Structures.** Table 1 contains the minimal RMS deviations of the unweighted Cartesian coordinates for various optimized structures compared to MP2/haTZ optimized structures. The first column of data shows the deviations associated with the HF/haTZ structures. As expected, HF/haTZ structures have large deviations from the MP2/haTZ structures. The second column of data in Table 1 reports the RMS deviations for the MP2/6-31G* optimized structures. Overall, MP2/6-31G* has improved accuracy compared to HF/haTZ methodology. Occasionally however, the MP2/6-31G* RMS values exceed those for the HF/haTZ structures. The values in the last two columns of Table 1 are appreciably smaller, indicating that the B3LYP/6-31+G(d,2p) and MP2/haTZ:HF/haTZ optimized structures deviate only slightly from the MP2/haTZ ones. The two-body:many-body approach consistently reproduces the MP2/haTZ structures more accurately than any other procedure.

Table 2 summarizes the results of Table 1 with the average and maximum RMS deviations associated with each method for each value of *n*. The second column lists the number of isomers used to compute the average (unless otherwise noted) . For example, the largest RMS deviation between the HF/haTZ and MP2/haTZ structures is 0.465 Å (for isomer BI1 of the water heptamer). In general, the average and maxium RMS deviations of the HF/haTZ and MP2/6-31G* approaches are comparable, with the later exhibiting slightly better performance overall. The average values are roughly 1 order of magnitude smaller for the B3LYP/6-31+G(d,2p) optimized structures. The last two columns of Table 2 list the average and maximum RMS deviations associated with the two-body:many-body fragmentation method employing MP2/haTZ for the high-level calculation and HF/haTZ for the low-level calculations. Regardless of the size of the cluster, this QM:QM fragmentation procedure yields the smallest average errors relative to the MP2/haTZ optimized structures. In fact the RMS deviations never exceed 0.038 Å .

**4.2. Comparison of Energetics.** Table 3 is similar to Table 1, but it reports energetic, rather than structural, deviations from the MP2/haTZ optimized structures (i.e., from the MP2/haTZ//MP2/haTZ energies). For example, the first column of data reports the MP2/haTZ//HF/haTZ errors associated with the

**Table 3. Errors Associated with MP2/haTZ Energies (in kcal mol$^{-1}$) Performed on Various Optimized Structures Relative to the MP2/haTZ//MP2/haTZ Values**

| method | HF | MP2 | B3LYP | MP2:HF |
|---|---|---|---|---|
| basis set | haTZ | 6-31G* | 6-31+G(d,2p) | haTZ |
| | | $(H_2O)_3$ | | |
| $C_1$ | 2.57 | 0.74 | 0.10 | 0.00 |
| $C_3$ | 2.59 | 0.97 | 0.11 | 0.00 |
| $C_{3h}$ | 2.27 | 0.25 | 0.10 | 0.00 |
| | | $(H_2O)_4$ | | |
| $S_4$ | 3.82 | 0.71 | 0.14 | 0.01 |
| $C_i$ | 3.83 | 0.78 | 0.15 | 0.01 |
| $C_4$ | 3.83 | 1.05 | 0.16 | 0.00 |
| $C_{4h}$ | 3.25 | 0.37 | 0.16 | 0.00 |
| | | $(H_2O)_5$ | | |
| $C_1$ | 4.81 | 0.87 | 0.19 | 0.01 |
| $C_5$ | 4.69 | 1.07 | 0.21 | 0.01 |
| $C_{5h}$ | 4.16 | 0.51 | 0.21 | 0.00 |
| | | $(H_2O)_6$ | | |
| prism | 6.47 | 0.79 | 0.25 | 0.01 |
| cage | 6.50 | 0.98 | 0.26 | 0.01 |
| book 1 | 6.18 | 1.15 | 0.23 | 0.01 |
| book 2 | 6.25 | [a] | 0.25 | 0.01 |
| bag | 6.32 | [b] | 0.24 | 0.01 |
| boat 1 | 5.72 | 1.34 | 0.25 | 0.01 |
| boat 2 | 5.64 | 1.22 | 0.25 | 0.01 |
| cyclic | 5.67 | 1.12 | 0.23 | 0.01 |
| | | $(H_2O)_7$ | | |
| A | 7.77 | 1.14 | 0.30 | 0.01 |
| B | 7.64 | 2.36 | 0.29 | 0.01 |
| C | 7.21 | 0.28 | 0.28 | 0.01 |
| D | 6.89 | 1.58 | 0.25 | 0.01 |
| PR2 | 7.82 | 1.02 | 0.31 | 0.01 |
| PR3 | 7.21 | 1.07 | 0.30 | 0.01 |
| CA1 | 7.07 | 1.09 | 0.28 | 0.01 |
| CA2 | 6.53 | 1.26 | 0.28 | 0.01 |
| CH1 | 7.20 | 1.21 | 0.28 | 0.01 |
| BI1 | 6.82 | 1.44 | 0.25 | 0.01 |
| CH2 | 7.20 | 2.20 | 0.27 | 0.01 |
| | | $(H_2O)_8$ | | |
| $C_1$a | 9.29 | 1.05 | 0.34 | 0.01 |
| $C_1$b | 9.36 | 1.03 | 0.35 | 0.02 |
| $C_1$c | 9.32 | 1.03 | 0.35 | 0.01 |
| $C_2$ | 9.65 | 0.78 | 0.39 | 0.01 |
| $C_i$ | 9.73 | 0.86 | 0.35 | 0.01 |
| $C_s$ | 9.53 | 1.01 | 0.35 | 0.02 |
| $D_{2d}$ | 9.47 | 1.17 | 0.35 | 0.02 |
| noncubic 1 | 9.13 | 1.83 | 0.41 | 0.02 |
| $S_4$ | 9.50 | 1.19 | 0.36 | 0.02 |
| | | $(H_2O)_9$ | | |
| $D_{2d}$DDh | 10.57 | 1.31 | 0.38 | 0.02 |
| $S_4$Dah 1 | 10.69 | 1.30 | 0.38 | 0.02 |

**Table 3. Continued**

| method | HF | MP2 | B3LYP | MP2:HF |
|---|---|---|---|---|
| basis set | haTZ | 6-31G* | 6-31+G(d,2p) | haTZ |
| $S_4$Dah 2 | 10.66 | 1.35 | 0.38 | 0.02 |
| $S_4$DDh 1 | 10.61 | 1.35 | 0.39 | 0.02 |
| $S_4$DDh 2 | 10.60 | 1.36 | 0.39 | 0.02 |
| $D_{2d}$Dah | 10.65 | 1.34 | 0.37 | 0.02 |
| $S_4$Danh 1 | 10.68 | 1.39 | 0.38 | 0.02 |
| $S_4$Danh 2 | 10.66 | 1.35 | 0.38 | 0.02 |
| | | $(H_2O)_{10}$ | | |
| PP1 | [c] | 1.30 | 0.38 | 0.00 |
| PP2 | 11.99 | 1.35 | 0.43 | 0.02 |
| PP3 | 12.03 | 1.37 | 0.41 | 0.01 |
| PP4 | 12.20 | 1.36 | 0.40 | 0.02 |
| PP5 | 12.03 | 1.41 | 0.43 | 0.02 |
| OB1 | 11.91 | 1.45 | 0.43 | 0.02 |
| OB2 | 11.94 | 1.47 | 0.44 | 0.01 |
| OB3 | 11.94 | 1.48 | 0.44 | 0.02 |
| DP1 | [d] | 1.42 | 0.41 | 0.02 |
| OB4 | 11.93 | 1.42 | 0.42 | 0.02 |
| OB5 | 11.94 | 1.98 | 0.43 | 0.02 |
| DP2 | 11.81 | 1.50 | 0.43 | 0.02 |
| OB6 | 11.95 | 1.51 | 0.43 | 0.02 |
| OB7 | 11.95 | 1.36 | 0.43 | 0.02 |
| OB8 | 11.94 | 1.38 | 0.42 | 0.02 |
| DP3 | 11.85 | 1.48 | 0.37 | 0.02 |
| DP4 | 11.72 | 1.44 | 0.29 | 0.01 |
| DP5 | 11.69 | 1.53 | 0.37 | 0.02 |
| OB9 | 12.03 | 1.90 | 0.43 | 0.02 |
| DP6 | 11.87 | 1.71 | 0.41 | 0.02 |
| DP7 | 11.33 | 1.65 | 0.41 | 0.02 |
| DP8 | 11.74 | 1.82 | 0.07 | 0.02 |
| OB10 | 11.92 | 2.98 | 0.42 | 0.01 |
| OB11 | 11.55 | 1.92 | 0.33 | 0.02 |
| DP10 | 11.75 | 1.63 | 0.41 | 0.01 |
| DP11 | 11.83 | 1.59 | 0.41 | 0.03 |
| C1 | 11.84 | 1.48 | 0.40 | 0.02 |
| C2 | 11.49 | 1.55 | 0.41 | 0.02 |
| C3 | 11.63 | 1.42 | 0.41 | 0.02 |

[a] Collapsed to prism structure. [b] Not located on the MP2/6-31G* PES. [c] Not located on the HF/haTZ PES. [d] Collapsed to DP2 structure.

total cluster energy compared to the MP2/haTZ//MP2/haTZ energies. The MP2/haTZ//HF/haTZ errors are always the largest, which is entirely consistent with the RMS deviations. In contrast, the MP2/haTZ//MP2/6-31G* errors are much smaller despite having RMS deviations comparable to the HF/haTZ optimized structures. The errors associated with the B3LYP/6-31+G(d,2p) structures are listed in the penultimate column, and they are significantly smaller than the errors associated with the HF/haTZ and MP2/6-31G* optimized structures. The last column of data shows the energetic errors associated with the two-body:many-body scheme. Structures optimized with the MP2:HF QM:QM fragmentation method and the haTZ basis set are typically one or two hundredths of a kcal mol$^{-1}$ above the MP2/haTZ optimized structures.

**Table 4. Average and Maximum Errors for MP2/haTZ Energies (in kcal mol$^{-1}$) Performed on Various Structures Relative to MP2/haTZ//MP2/haTZ Values for $(H_2O)_n$ Clusters with $n$ = 3−10**

| | | HF/haTZ | | MP2/6-31G* | | B3LYP/6-31+G(d,2p) | | MP2:HF/haTZ | |
|---|---|---|---|---|---|---|---|---|---|
| $n$ | no. | avg | max | avg | max | avg | max | avg | max |
| 3 | 3 | 2.48 | 2.59 | 0.65 | 0.97 | 0.10 | 0.11 | 0.00 | 0.00 |
| 4 | 4 | 3.68 | 3.83 | 0.73 | 1.05 | 0.15 | 0.16 | 0.00 | 0.01 |
| 5 | 3 | 4.55 | 4.81 | 0.81 | 1.07 | 0.21 | 0.21 | 0.01 | 0.01 |
| 6 | 8 | 6.09 | 6.50 | 1.10[a] | 1.34[a] | 0.24 | 0.26 | 0.01 | 0.01 |
| 7 | 11 | 7.21 | 7.82 | 1.45 | 2.36 | 0.28 | 0.31 | 0.01 | 0.02 |
| 8 | 9 | 9.44 | 9.73 | 1.11 | 1.83 | 0.36 | 0.41 | 0.01 | 0.02 |
| 9 | 8 | 10.64 | 10.69 | 1.34 | 1.39 | 0.38 | 0.39 | 0.02 | 0.02 |
| 10 | 29 | 11.84[b] | 12.20 | 1.58 | 2.98 | 0.40 | 0.44 | 0.02 | 0.03 |

[a] Excludes the bag and book 2 isomers. [b] Excludes the PP1 and DP1 isomers.

Again, average and maximum errors are tabulated to help summarize all of the data in Table 3. For example, the data in Table 4 show that the errors associated with the HF/haTZ structures optimized structures increase with the size of the cluster and grow as large as 12.20 kcal mol$^{-1}$ (for the PP4 isomer of the water decamer). The energetic errors associated with the MP2/6-31G* optimized structures also tend to increase with the value of $n$ but do not exceed 2.98 kcal mol$^{-1}$ (for isomer OB10 of the water decamer). The combination of the B3LYP density functional with the 6-31+G(d,2p) basis set appears to be a good way to quickly and reliably identify low-lying structures of $(H_2O)_n$ clusters. The largest MP2/haTZ//B3LYP/6-31+G(d,2p) error is only 0.44 kcal mol$^{-1}$ (for both OB2 and OB3 structures of the water decamer). The two-body:many-body integrated fragmentation technique for noncovalent clusters provides even more accurate results. The errors associated with the structures optimized with the MP2:HF method and the haTZ basis set never exceed 0.03 kcal mol$^{-1}$ (for DP11 isomer of the water decamer). The average error for the MP2:HF fragmentation method is 0.01 kcal mol$^{-1}$ for all of 75 water clusters examined. These two-body:many-body results are particularly encouraging for certain pathological cases where water clusters are virtually isoenergetic and separated by less than 0.10 kcal mol$^{-1}$. For example, the MP2 complete basis set limit interaction energies for the prism and cage isomers of the water hexamer are separated electronically by only 0.06 kcal mol$^{-1}$.[10,21]

**4.3. Efficiency and Convergence.** In general, we have found that the convergence of geometry optimizations for the MP2:HF procedure is virtually identical to that of the MP2 method. For well-behaved cases, the MP2:HF optimization converges in a similar number cycles, typically ±10%, as the corresponding MP2 optimization (e.g., ± 2 iterations for a 20-step optimization). To demonstrate this behavior, both MP2 and MP2:HF geometry optimizations were started from the B3LYP/6-31+G(d,2p) optimized structure of the $C_1$a isomer of $(H_2O)_8$. The corresponding RMS gradients (in $E_h$ $a_0^{-1}$) and relative electronic energies [in millihartree ($mE_h$) with respect to the optimized structures] are shown in Figure 1. For this system, the MP2 optimization converges quickly (within 20 iterations), and the progression of the MP2:HF procedure is virtually identical. Only for iterations 8 and 9 is there any noticible difference between the MP2 and MP2:HF optimizations. It should be noted, however, that when it is difficult to

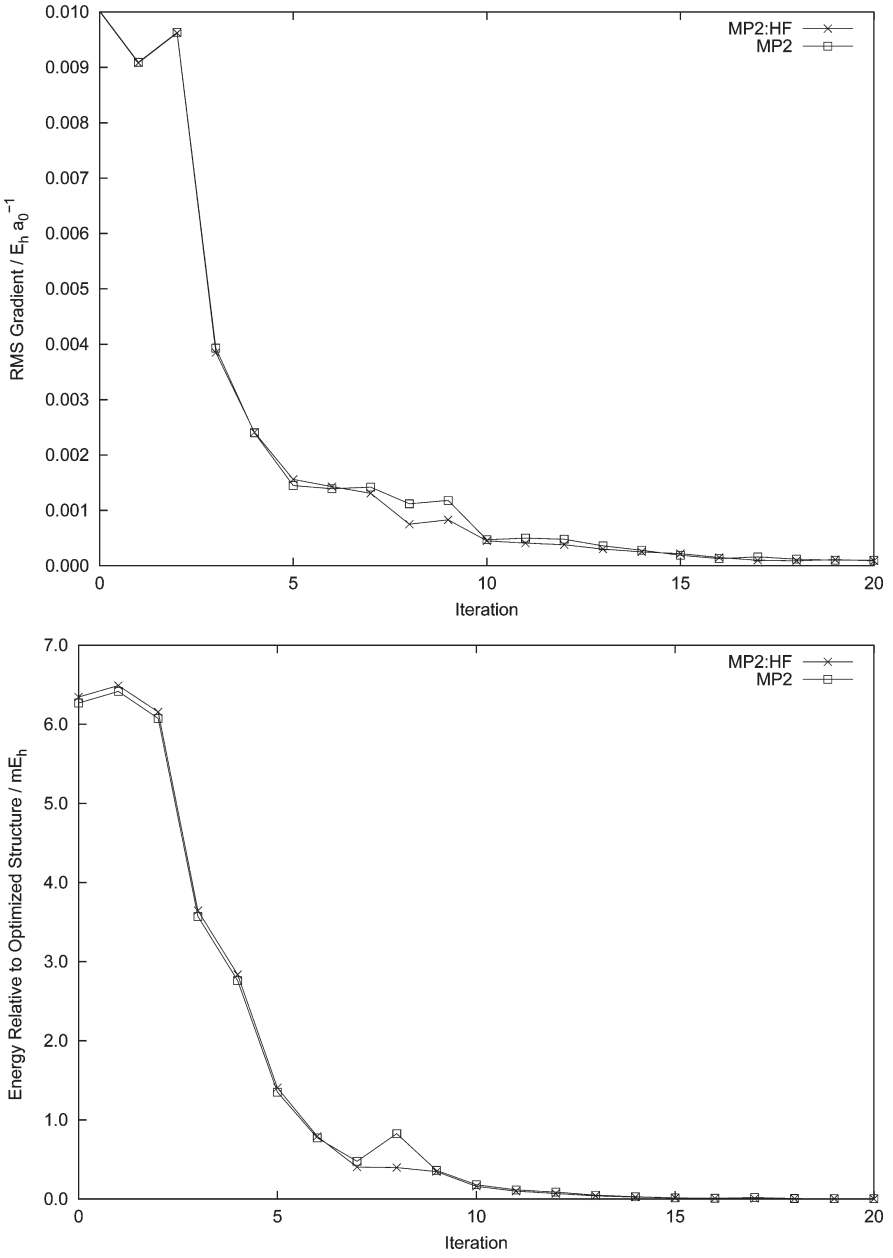


**Figure 1.** RMS gradients and relative energies during MP2 and MP2:HF geometry optimizations of the $C_1$a isomer of the water octamer.

converge the high-level geometry optimization, as is common for weakly bound noncovalent clusters, the same problem should be expected for the corresponding two-body:many-body QM:QM geometry optimization.

The efficiency of the two-body:many-body gradient computations relative to the high-level method depends not only on the size and nature of the cluster being examined but also on the methods, basis sets, and software programs used for the high- and low-level calculations. To provide some measurement of the efficiency of our approach, we recomputed the MP2 and MP2:HF gradients for the $C_1$a isomer of $(H_2O)_8$ and the PP1 isomer of $(H_2O)_{10}$ with the MPQC program on a workstation equipped with two quad-core Opteron 2.4 GHz 2378 processors and 32 GB of memory. The wall times (in minutes) are reported in Table 5. (Note that no timings reported here were obtained with Gaussian.) The first column of data has been labeled "MPQC:MPQC" to denote that both the MP2 and HF computations were perfomed with the MPQC software package. When computed in this manner, the MP2:HF gradient is approximately twice as fast as the canonical MP2 gradient calculation. Roughly 70% of the wall time in these MP2:HF computations is spent evaluating the low-level gradient for the complex. Efficiency can be further improved by using a program with faster parallel HF first derivatives. The last column of data (with the "MPQC:PQS" heading) contains the wall times obtained when PQS[61] is used to compute the HF gradients and MPQC is only used for the MP2 gradients. PQS dramatically decreases the time for the HF gradients (by a factor of $\approx$8), which increases the speedups associated with the MP2:HF computations by a factor of 3. In both columns, the efficiency of the two-body:many-body procedure increases with the size of the cluster. Spatial and energetic thresholds are expected to further improve efficiency because distance-based cutoffs have yielded

**Table 5. Typical Wall Times (in minutes) Associated with the Two-Body:Many-Body MP2:HF Gradient Calculations and Speedups Relative to the MP2 Gradient Computed with MPQC**

| | | MP2:HF | MP2:HF |
|---|---|---|---|
| calculation(s) | | MPQC: MPQC | MPQC: PQS |
| | $C_1$a Isomer of $(H_2O)_8$ | | |
| lo-level | 8 fragments | <1 | <1 |
| hi-level | 8 fragments | 1 | 1 |
| lo-level | 28 pairs | 23 | 6 |
| hi-level | 28 pairs | 47 | 47 |
| lo-level | 1 complex | 144 | 18 |
| total | | 215 | 72 |
| speedup (relative to 376 min)[a] | | 1.7 | 5.2 |
| | PP1 Isomer of $(H_2O)_{10}$ | | |
| lo-level | 8 fragments | <1 | <1 |
| hi-level | 8 fragments | 1 | 1 |
| lo-level | 28 pairs | 36 | 9 |
| hi-level | 28 pairs | 72 | 72 |
| lo-level | 1 complex | 267 | 34 |
| total | | 376 | 115 |
| speedup (relative to 887 min)[a] | | 2.4 | 7.7 |

[a] Wall time for MP2 gradient with MPQC.

very promising results for the closely related molecules-in-molecules method.[51]

## 5. CONCLUSIONS

Analytic gradient techniques for the two-body:many-body fragmentation method for weakly bound clusters were used to optimize the geometries of more than 70 water clusters ranging in size from $(H_2O)_3$ to $(H_2O)_{10}$. In this application, MP2/haTZ was used as the high-level method to compute the one- and two-body interactions, while HF/haTZ was employed as the low-level method to recover the higher-order ($\geq$three-body) interactions. This procedure proved to be quite efficient because the largest MP2 computations associated with the MP2:HF calculations involve a pair of water molecules (i.e., a dimer), regardless of the size of the cluster. Consequently, the HF/haTZ computation on the entire cluster was always the rate determining step in these two-body:many-body fragmentation calculations. Structures optimized with this QM:QM fragmentation procedure were compared to those obtained from conventional MP2/haTZ optimizations using two different metrics, the minimum RMS deviation of unweighted Cartesian coordinates and the MP2/haTZ energy. The two-body:many-body optimized structures were virtually identical to those from the MP2/haTZ optimizations. On average, the structures optimized with these two methods were within 0.01 kcal $mol^{-1}$ of each other on the MP2/haTZ PES, and they never differed by more than 0.03 kcal $mol^{-1}$ . For comparison, HF/haTZ and MP2/6-31G* optimized structures deviated by as much as 12.20 and 2.98 kcal $mol^{-1}$, respectively, from the MP2/haTZ structures. This work also demonstrated that the B3LYP/6-31+G(d,2p) structures did not differ from the MP2/haTZ ones by more than 0.44 kcal $mol^{-1}$ on the MP2/haTZ PES.

## ■ ASSOCIATED CONTENT

**Supporting Information.** Tables of Cartesian coordinates for the MP2/haTZ-optimized structures from this work are included. This material is available free of charge via the Internet at http://pubs.acs.org.

## ■ AUTHOR INFORMATION

**Corresponding Author**
*E-mail: tschumpr@olemiss.edu.

## ■ ACKNOWLEDGMENT

We acknowledge the Mississippi Center for Super Computing Research for CPU time and the National Science Foundation for funding (CHE-0957317 and EPS-0903787).

## ■ REFERENCES

(1) Castleman, A.; Bowen, K. *J. Phys. Chem.* **1996**, *100*, 12911–12944.
(2) Bačić, Z.; Miller, R. E. *J. Phys. Chem.* **1996**, *100*, 12945–12959.
(3) Jeffrey, G. A. *An Introduction to Hydrogen Bonding*; Oxford University Press: Oxford, England, 1997.
(4) Schuster, P.; Wolschann, P. *Monat. Chem.* **1999**, *130*, 947–960.
(5) Ludwig, R. *Angew. Chem., Int. Ed. Engl.* **2001**, *40*, 1808–1827.
(6) Steiner, T. *Angew. Chem., Int. Ed. Engl.* **2002**, *41*, 48–76.
(7) Černý, J.; Hobza, P. *Phys. Chem. Chem. Phys.* **2007**, *9*, 5281–5388.
(8) Klopper, W.; Schuetz, M. *Ber. Bunsen. Phys. Chem.* **1995**, *99*, 469–473.
(9) Klopper, W.; Quack, M.; Suhm, M. A. *Mol. Phys.* **1998**, *94*, 105–116.
(10) Xantheas, S. S.; Burnham, C. J.; Harrison, R. J. *J. Chem. Phys.* **2002**, *116*, 1493–1499.
(11) Sinnokrot, M.; Valeev, E.; Sherrill, C. *J. Am. Chem. Soc.* **2002**, *124*, 10887–10893.
(12) Hobza, P. *Annu. Rep. Prog. Chem., Sect. C: Phys. Chem.* **2004**, *100*, 3–27.
(13) Zhao, Y.; Truhlar, D. G. *J. Chem. Theory Comput.* **2005**, *1*, 415–432.
(14) Jurečka, P.; Šponer, J.; Černý, J.; Hobza, P. *Phys. Chem. Chem. Phys.* **2006**, *8*, 1985–1993.
(15) Boese, A.; Martin, J.; Klopper, W. *J. Phys. Chem. A* **2007**, *111*, 11122–11133.
(16) Tschumper, G. S.; Leininger, M. L.; Hoffman, B. C.; Valeev, E. F.; Schaefer, H. F.; Quack, M. *J. Chem. Phys.* **2002**, *116*, 690–701.
(17) Anderson, J. A.; Crager, K.; Fedoroff, L.; Tschumper, G. S. *J. Chem. Phys.* **2004**, *121*, 11023–11029.
(18) Hopkins, B. W.; Tschumper, G. S. *J. Phys. Chem. A* **2004**, *108*, 2941–2948.
(19) Copeland, K. L.; Anderson, J. A.; Farley, A. R.; Cox, J. R.; Tschumper, G. S. *J. Phys. Chem. B* **2008**, *112*, 14291–14295.
(20) ElSohly, A. M.; Hopkins, B. W.; Copeland, K. L.; Tschumper, G. S. *Mol. Phys.* **2009**, *107*, 923–928.
(21) Bates, D. M.; Tschumper, G. S. *J. Phys. Chem. A* **2009**, *113*, 3427–3708.
(22) Christie, R. A.; Jordan, K. D. *n*-Body Decomposition Approach to the Calculation of Interaction Energies of Water Clusters. In *Intermolecular Forces and Clusters II*; Wales, D. J., Ed.; Springer: Germany, 2005; Vol. 116, pp 27−41.
(23) Kitaura, K.; Ikeo, E.; Asada, T.; Nakano, T.; Uebayasi, M. *Chem. Phys. Lett.* **1999**, *313*, 701–706.
(24) Nakano, T.; Kaminuma, T.; Sato, T.; Akiyama, Y.; Uebayasi, M.; Kitaura, K. *Chem. Phys. Lett.* **2000**, *318*, 614–618.
(25) Fedorov, D. G.; Kitaura, K. *J. Phys. Chem. A* **2007**, *111*, 6904–6914.
(26) Fedorov, D. G.; Ishimura, K.; Ishida, T.; Kitaura, K.; Pulay, P.; Nagase, S. *J. Comput. Chem.* **2007**, *28*, 1476–1484.

(27) Hirata, S.; Valiev, M.; Dupuis, M.; Xantheas, S. S.; Sugiki, S.; Sekino, H. *Mol. Phys.* **2005**, *103*, 2255–2265.
(28) Sakai, S.; Morita, S. *J. Phys. Chem. A* **2005**, *109*, 8424–8429.
(29) Dahlke, E.; Truhlar, D. *J. Chem. Theory Comput.* **2007**, *3*, 46–53.
(30) Dahlke, E.; Truhlar, D. *J. Chem. Theory Comput.* **2007**, *3*, 1342–1348.
(31) Dahlke, E.; Leverentz, H.; Truhlar, D. *J. Chem. Theory Comput.* **2008**, *4*, 33–41.
(32) Imamura, A.; Aoki, Y.; Maekawa, K. *J. Chem. Phys.* **1991**, *95*, 5419–5431.
(33) Zhang, D. W.; Zhang, J. Z. H. *J. Chem. Phys.* **2003**, *119*, 3599–3605.
(34) Jiang, N.; Ma, J.; Jiang, Y. *J. Chem. Phys.* **2006**, *124*, 114112.
(35) Gadre, S. R.; Shirsat, R. N.; Limaye, A. C. *J. Chem. Phys.* **1994**, *98*, 9103–9169.
(36) Sæbø, S.; Pulay, P. *Chem. Phys. Lett.* **1985**, *113*, 13–18.
(37) Day, P. N.; Jensen, J. H.; Gordon, M. S.; Webb, S. P.; Stevens, W. J.; Krauss, M.; Garmer, D.; Basch, H.; Cohen, D. *J. Chem. Phys.* **1996**, *105*, 1968–1986.
(38) Rauhut, G.; Pulay, P.; Werner, H. J. *J. Comput. Chem.* **1998**, *19*, 1241–1254.
(39) Li, S.; Ma, J.; Jiang, Y. *J. Comput. Chem.* **2002**, *23*, 237–244.
(40) Min, D.; Yang, W. *J. Chem. Phys.* **2008**, *128*, 094106.
(41) Li, W.; Piecuch, P.; Gour, J. R.; Li, S. *J. Chem. Phys.* **2009**, *131*, 114109.
(42) Gordon, M. S.; Mullin, J. M.; Pruitt, S. R.; Roskop, L. B.; Slipchenko, L. V.; Boatz, J. A. *J. Phys. Chem. B* **2009**, *113*, 9646–9663.
(43) Hopkins, B. W.; Tschumper, G. S. *J. Comput. Chem.* **2003**, *24*, 1563–1568.
(44) Hopkins, B. W.; Tschumper, G. S. *Mol. Phys.* **2005**, *103*, 309–315.
(45) Hopkins, B. W.; Tschumper, G. S. *Chem. Phys. Lett.* **2005**, *407*, 362–367.
(46) Tschumper, G. S. *Chem. Phys. Lett.* **2006**, *427*, 185–191.
(47) Maseras, F.; Morokuma, K. *J. Comput. Chem.* **1995**, *16*, 1170–1179.
(48) Ganesh, V.; Dongare, R. K.; Balanarayan, P.; Gadre, S. R. *J. Chem. Phys.* **2006**, *125*, 104109.
(49) Li, W.; Li, S.; Jiang, Y. *J. Phys. Chem. A* **2007**, *111*, 2193–2199.
(50) Hua, W.; Fang, T.; Li, W.; Yu, J.-G.; Li, S. *J. Phys. Chem. A* **2008**, *112*, 10864–10872.
(51) Mayhall, N. J.; Raghavachari, K. *J. Chem. Theory Comput.* **2011**, *7*, 1336–1343.
(52) Bates, D. M.; Janowski, T.; Smith, J. R.; Tschumper, G. S. *J. Chem. Phys.* **2011**, *135*, 012345.
(53) Janssen, C. L.; Nielsen, I. B.; Leininger, M. L.; Valeev, E. F.; Seidl, E. T. *The Massively Parallel Quantum Chemistry Program (MPQC)*, version 2.3.1; Sandia National Laboratories: Livermore, CA, 2004; http://www.mpqc.org.
(54) ElSohly, A. M.; Shaw, C. L.; Guice, M. E.; Smith, B. D.; Tschumper, G. S. *Mol. Phys.* **2007**, *105*, 2777–2782.
(55) Dahlke, E. E.; Olson, R. M.; Leverentz, H. R.; Truhlar, D. G. *J. Phys. Chem. A* **2008**, *112*, 3976–3984.
(56) Shields, R. M.; Temelso, B.; Archer, K. A.; Morrell, T. E.; Shields, G. C. *J. Phys. Chem. A* **2010**, *114*, 11725–11737.
(57) Frisch, M. J.; Trucks, G. W.; Schlegel, H. B.; Scuseria, G. E.; Robb, M. A.; Cheeseman, J. R.; Montgomery, J. R., Jr.; Vreven, T.; Kudin, K. N.; Burant, J. C.; Millam, J. M.; Iyengar, S. S.; Tomasi, J.; Barone, V.; Mennucci, B.; Cossi, M.; Scalmani, G.; Rega, N.; Petersson, G. A.; Nakatsuji, H.; Hada, M.; Ehara, M.; Toyota, K.; Fukuda, R.; Hasegawa, J.; Ishida, M.; Nakajima, T.; Honda, Y.; Kitao, O.; Nakai, H.; Klene, M.; Li, X.; Knox, J. E.; Hratchian, H. P.; Cross, J. B.; Bakken, V.; Adamo, C.; Jaramillo, J.; Gomperts, R.; Stratmann, R. E.; Yazyev, O.; Austin, A. J.; Cammi, R.; Pomelli, C.; Ochterski, J. W.; Ayala, P. Y.; Morokuma, K.; Voth, G. A.; Salvador, P.; Dannenberg, J. J.; Zakrzewski, V. G.; Dapprich, S.; Daniels, A. D.; Strain, M. C.; Farkas, O.; Malick, D. K.; Rabuck, A. D.; Raghavachari, K.; Foresman, J. B.; Ortiz, J. V.; Cui, Q.; Baboul, A. G.; Clifford, S.; Cioslowski, J.; Stefanov, B. B.; Liu, G.; Liashenko, A.; Piskorz, P.; Komaromi, I.; Martin, R. L.; Fox, D. J.; Keith, T.; Al-Laham, M. A.; Peng, C. Y.; Nanayakkara, A.; Challacombe, M.; Gill, P. M. W.; Johnson, B.; Chen, W.; Wong, M. W.; Gonzalez, C.; Pople, J. A. *Gaussian 03*, revision E.01; Gaussian, Inc.: Wallingford, CT, 2003.
(58) Frisch, M. J.; Trucks, G. W.; Schlegel, H. B.; Scuseria, G. E.; Robb, M. A.; Cheeseman, J. R.; Scalmani, G.; Barone, V.; Mennucci, B.; Petersson, G. A.; Nakatsuji, H.; Caricato, M.; Li, X.; Hratchian, H. P.; Izmaylov, A. F.; Bloino, J.; Zheng, G.; Sonnenberg, J. L.; Hada, M.; Ehara, M.; Toyota, K.; Fukuda, R.; Hasegawa, J.; Ishida, M.; Nakajima, T.; Honda, Y.; Kitao, O.; Nakai, H.; Vreven, T.; Montgomery, J. A., Jr.; Peralta, J. E.; Ogliaro, F.; Bearpark, M.; Heyd, J. J.; Brothers, E.; Kudin, K. N.; Staroverov, V. N.; Kobayashi, R.; Normand, J.; Raghavachari, K.; Rendell, A.; Burant, J. C.; Iyengar, S. S.; Tomasi, J.; Cossi, M.; Rega, N.; Millam, J. M.; Klene, M.; Knox, J. E.; Cross, J. B.; Bakken, V.; Adamo, C.; Jaramillo, J.; Gomperts, R.; Stratmann, R. E.; Yazyev, O.; Austin, A. J.; Cammi, R.; Pomelli, C.; Ochterski, J. W.; Martin, R. L.; Morokuma, K.; Zakrzewski, V. G.; Voth, G. A.; Salvador, P.; Dannenberg, J. J.; Dapprich, S.; Daniels, A. D.; Farkas, O.; Foresman, J. B.; Ortiz, J. V.; Cioslowski, J.; Fox, D. J. *Gaussian 09*, revision A.2; Gaussian, Inc.: Wallingford, CT, 2009.
(59) Ponder, J. W. *TINKER - Software tools for molecular design*, version 5.1.09; Washington University School of Medicine: Saint Louis, MO, 2009.
(60) Qian, P.; Song, W.; Lu, L.; Yang, Z. *Int. J. Quantum Chem.* **2010**, *110*, 1923–1937.
(61) *PQS*, version 4.0; Parallel Quantum Solutions: Fayetteville, Arkansas;http://www.pqs-chem.com.